Am J Transl Res 2016;8(4):1826-1837
www.ajtr.org /ISSN:1943-8141/AJTR0023598

Original Article

MicroRNA-544 inhibits glioma proliferation, invasion and migration but induces cell apoptosis by targeting PARK7

Shiguang Jin[1], Yan Dai[1], Cheng Li[2], Xiao Fang[2], Huijing Han[2], Daxin Wang[2]

[1]The Second Xiangya Hospital of Central South University, Changsha 410011, Hunan, China; [2]Northern Jiangsu People's Hospital, Yangzhou, Jiangsu 225001, China

Received January 8, 2016; Accepted February 3, 2016; Epub April 15, 2016; Published April 30, 2016

Abstract: Glioma is a common type of primary brain tumor. The survival rate in people with malignant gliomas is extremely low associated with the lack of effective treatment. Here, we firstly observed that miR-544 expression is downregulated in glioma tissues and its overexpression in glioma cell line dramatically reduces cell proliferation, migration and invasion. In addition, we found that the tumor growth in nude mouse was as well inhibited by miR-544 overexpressed in glioma cell. Our further investigation showed that the inhibitor role of miR-544 in tumor development was related to the downregulated expression of Park7 gene which has been demonstrated as a functional downstream target of miR-544. Thus, our discovery suggested that miR-544 might used as a therapeutic reagent for the treatment of glioma in the future.

Keywords: microRNA, glioma, cell growth, invasion, migration, PARK7

Introduction

Gliomas have been defined as the tumors starting in brain or spine [1]. They comprise 30% of all brain and central nervous system tumors and 80% of all malignant brain tumors [2]. Brain tumors are relatively rare events but the survival rates of the majority of malignant gliomas are very low. The difficulties in treating the tumors are attributed to their features including unobvious clinical, radiologic or morphologic forewarning and their infiltrating natures [3, 4]. Furthermore, the obstacles including multidrug resistance, radioresistance, an impermeable blood-brain barrier, a lack of preclinical models, and a rudimentary understanding of neurooncogenetics prevent patients from effective treatments and improved survivals [5]. A more efficient treatment strategy for glioma is urgently required.

A microRNA consisting of 20~22 nucleotides belongs to a class of non-coding RNA molecular which is involving the regulation of gene expression in a posttranscriptional manner [6, 7]. MicroRNAs have been reported to regulate different biological processes such as cell migration, invasion, proliferation, and apoptosis [8-11]. The roles of miRNAs in the regulation of glioma development have been described since their dysregulation were observed in glioblastoma using microarray analysis in 2005 [12]. MiR-21 has been revealed to work as an antiapoptotic factor by targeting a network of p53; MiR-10b regulated cell cycle and programmed cell death via regulation of Bim, TFAP2C, p16, and p21 [13, 14]; The increased level of miR-218 led to the reduction of cell migration, invasion, proliferation and stem-like qualities by inhibiting the oncogene Bmi1 expressing [15]; MiR-195 plays an important role in inhibiting the proliferation of glioma cells by downregulating expression of cyclin D1 and cyclin E1 [16]; miR-137 inhibits the growth of glimas cells by directly targeting Rac1 [17]; miR-16 functions as a tumor suppressor gene in glioma growth and invasiveness through inhibition of BCL2 and the NF-KB1/MMP-9 signaling pathway [18]. In this study, we discovered that the overexpression of miR-544 which is expressed at a low level in glioma cells inhibits the cell proliferation, migration and invasion through downregulating the PARK7 expression by targeting its 3'UTR.

Methods and materials

Glioma tissues

24 pairs of cervical cancer tissue and the adjacent normal tissue were obtained from Department of Pathology, Norman Bethune School of Medicine, Jilin University. All of the samples were obtained with the patients' informed consent and approved by the Ethics Committee of Department of Pathology, Norman Bethune School of Medicine, Jilin University.

Cell culture

Glioma cell lines U87-2M1, SW1088, U87, T98G, U251 and U138 were grown in DMEM medium supplemented with 10% fetal bovine serum (FBS). Cells were maintained in a humidified atmosphere at 37°C with 5% CO_2.

The predication of miRNA targeting gene

The miR-544 targets were predicted on the calculations of mirSVR scores by the computer-aided algorithms of PicTar and TargetScan Release 5.1

Quantitative RT-PCR

Total RNA in glioma cells was extracted using Trizol reagent and precipitated with buffer containing 2.5 volumes of ethanol. The RNA was dissolved in TE solution (10 mM Tris-Hcl 7.5, 0.1 mM EDTA) and further treated with RNase-free DNase I (Takara, Japan). The RNA was recovered using phenol/chloroform extraction followed by ethanol precipitation. The RNA concentration was estimated by measuring the absorbance at 260 nm using a NanoDrop 2000c (Thermo Scientific). The cDNA was synthesized using RT primer and SuperScript III reverse transcriptase following the manufacturer's instructions (Takara, Japan). Quantitative RT-PCR was performed using iQ™5 Multicolor Real-Time PCR Detection system (BioRad) with Realtime PCR Master Mix (SYBR Green, Toyobo, Osaka, Japan). GAPDH was chosen as the endogenous control in the assay.

3-(4, 5-dimethylthiazol-2-yl)-2, 5-diphenyltetrazolium bromide (MTT) assays

U87-2M1 and SW1088 cells with the concentration of 10^4 per well were seeded in a 96-well plate. According to the manufacture's protocol, miRNA mimic, negative control RNA or eukaryotic expression plasmids were transfected into the cell using Lipofectamine 2000 at the next day. The cells were cultured at 37°C in transfection media for 6 hours. And then the media was replaced by complete medium containing MTT (final concentration, 250 μg/mL) for the following assays. Plates were incubated for an additional 12 hours, 24 hours and 48 hours respectively. The trapped MTT crystals in cells were solubilized in 200 μL DMSO at 37°C for 15 min. Absorbance was determined in a microtiter plate reader (Molecular Devices, Menlo Park, CA) at 570 m, with 650 nm as the reference wavelength. All experiments were performed in triplicate.

Colony formation assay

For colony formation assays, the cells were harvested and seeded at a density of 200 cells per well in 12-well plates and incubated at 37°C and 5% CO_2 in a humidified incubator for 2 weeks. During colony growth, the culture medium was replaced every 3 days. The colony number in each well was counted and calculated.

Fluorescent reporter assay

Glioma cells were cotransfected using 0.2 μg of Luciferase reporter vector with a wild-type or mutant PARK7 3'UTR in 48-well plates and miR-544 mimics or miR-controls. The assay was normalized with 0.05 μg of the red fluorescent protein expression vector pDsRed2-N1 (Clontech, Mountain View, CA, USA). The cells were lysed with RIPA lysis buffer (0.15 M NaCl, 0.05 M Tris/HCl pH 7.2, 1% Triton X-100, 0.1% SDS) 48 hours later. The fluorescence intensities of Luciferase and red fluorescent protein were detected with an F-4500 Fluorescence Spectrophotometer (Hitachi, Tokyo, Japan).

Flow cytometry analysis

Glioma cells were harvested using trypsinization, washed in ice-cold PBS, and then fixed in 80% ice-cold ethanol in PBS. Before staining, cells were sedimented in a chilled centrifuge and resuspended in cold PBS to the concentration of ~10^4 cells. Bovine pancreatic RNase (Sigma-Aldrich, USA) was added to a final concentration of 2 mg/ml, and cells were incubated at 37°C for 30 min. For the detection of cell

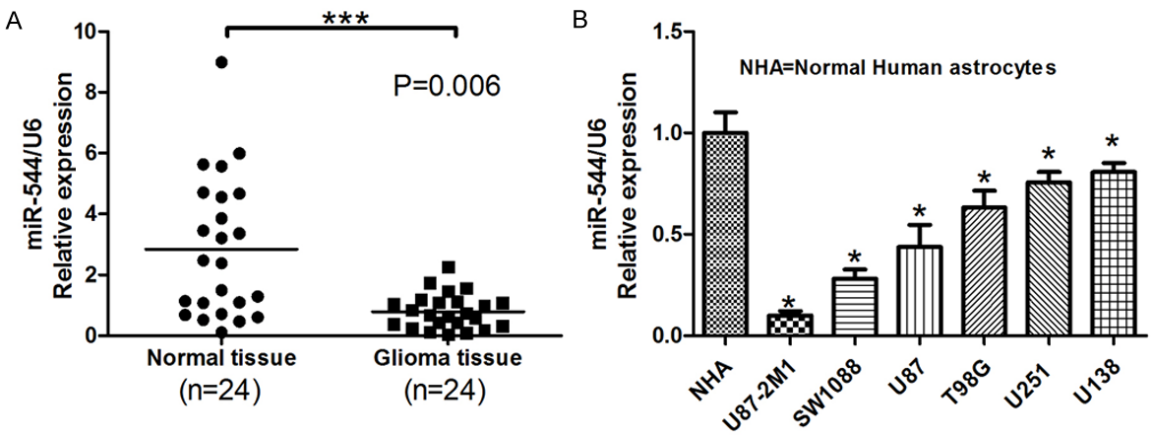

Figure 1. MiR-554 was downregulated in glioma tissues and cell lines. A. The relative levels of miR-544 in 24 cases of glioma tissues and their matched adjacent normal tissues were determined using U6 as internal controls in real-time RT-PCR assays. Each bar represents the mean of three independent experiments. *** means P<0.001. B. The relative levels of miR-544 normalized to U6 were measured in normal human astrocytes and six glioma cell lines, U87-2M1, SW1088, U87, T98G, U251 and U138. NHA: normal human astrocytes. Error bars represent SEM. * means P<0.05 vs. Normal.

cycle distribution, the cells were staining with 20 mg/ml of propidiumiodide (Sigma-Aldrich, USA) for 20 min at room temperature. In cell apoptosis assays, the cells were labeled using the Annexin V-FITC apoptosis detection kit (Invitrogen Corporation, California, USA) as described by the manufacturer's instructions. The cell cycle profiles and the cell apoptotic rates of the cells were quantified using a Flow cytometry (Beckman Coulter Corp., CA, USA).

Transwell assays

For transwell migration assays, 10^5 of cells were suspended in medium without serum and placed on the top side of polycarbonate Transwell the filters without Matrigel in the upper chamber of the QCM™ 24-Well Cell Invasion Assay (Cell Biolabs, INC, USA & Canada) and the medium without serum was used in the lower chamber. For the invasion assays, the experimental procedures were the similar to that for migration assays except that the filters with Matrigel is instead of the one without Matrigel. The cells were incubated at 37°C for 8 hours in migration assays or 48 hours in invasion assays, respectively. The cells in the top chambers were removed with cotton swabs. The migrated and invaded cells on the lower membrane surface were washed with PBS buffer twice and fixed in in 4% paraformaldehyde for 30 min. The well was stained with 0.1% crystal violet for 20 min after another repeat washing using PBS buffer. Following washing in ddH_2O more than three times, the membrane was dried, and observed under a light microscope. The assays were performed in triplets and the data were presented as the means ±standard error of mean (SEM).

Xenografted tumor model

7 pairs of the BALB/c nude mice were inoculated subcutaneously glioma cells of 3.0×10^6 infected with miR-544 mimics or miR-controls in the right dorsal flank per mouse. Tumors were examined every 5 days; length, width, and thickness measurements were obtained with calipers and tumor volumes were calculated. Tumor volume was calculated using the equation $(L*W^2)/2$. On day 25, then animals were killed, tumors were excised and weighed. All the animal assays were approved by the Ethics Committee of 1. The second xiangya hospital of central south university.

Statistical analysis

Data are presented as the mean ± standard deviation (SD). Student's t-test was used to evaluate significant differences, with $P<0.05$ considered statistically significant.

Results

The expression of miR-544 was downregulated in glioma tissues

The levels of miR-544 expressed in 24 cases of glioma tissues and their matched adjacent tis-

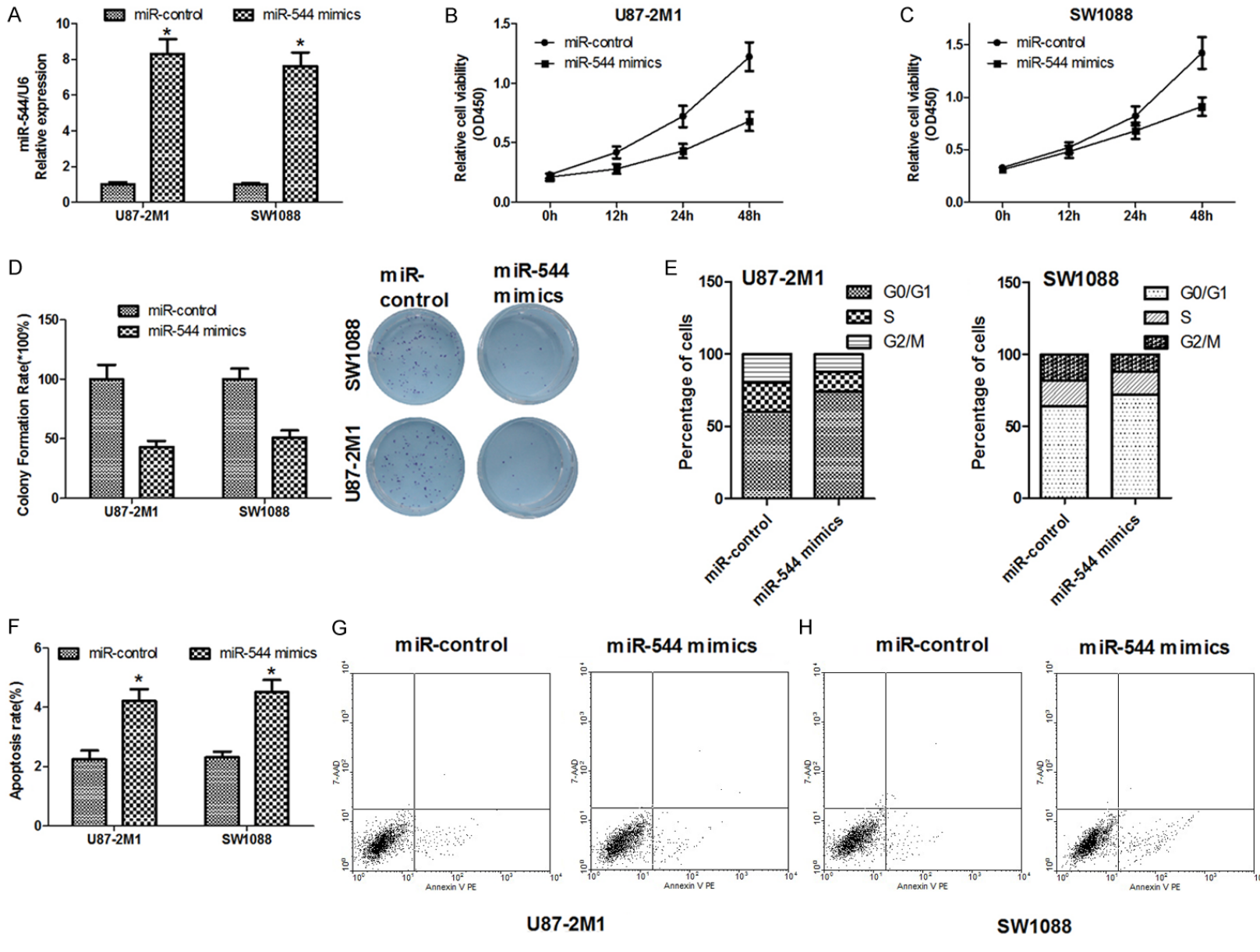
A
miR-control
miR-544 mimics
miR-544/U6 Relative expression
U87-2M1
SW1088
B
U87-2M1
miR-control
miR-544 mimics
Relative cell viability (OD450)
0h
12h
24h
48h
C
SW1088
miR-control
miR-544 mimics
Relative cell viability (OD450)
0h
12h
24h
48h
D
miR-control
miR-544 mimics
Colony Formation Rate(*100%)
U87-2M1
SW1088
miR-control
miR-544 mimics
SW1088
U87-2M1
E
U87-2M1
G0/G1
S
G2/M
Percentage of cells
miR-control
miR-544 mimics
SW1088
G0/G1
S
G2/M
Percentage of cells
miR-control
miR-544 mimics
F
miR-control
miR-544 mimics
Apoptosis rate(%)
U87-2M1
SW1088
G
miR-control
miR-544 mimics
7-AAD
Annexin V PE
U87-2M1
H
miR-control
miR-544 mimics
7-AAD
Annexin V PE
SW1088

Figure 2. Overexpression of miR-544 inhibits the proliferation but induces the apoptosis of the glioma cells in vitro. A. The relative levels of miR-544 normalized to U6 in two glioma cell lines, U87-2M1 and SW1088 were detected after the cells transfected with miR-544 mimics or miR-control using real-time RT-PCR. B. The relative cell viability in U87-2M1 cells was detected after the cells transfected with miR-544 mimics or miR-control using MTT assays. C. The relative cell viability in SW1088 cells was detected after the cells transfected with miR-544 mimics or miR-control using MTT assays. D. The colony formation of miR-544-U87-2M1 cells and that of miR-544-SW1088 cells were quantified and compared with that of the glioma cells transfected with miR-control in their respective groups (Left). The corresponding representative micrographs located on the right. E. The cell cycle distributions of the U87-2M1 cells transfected with miR-544 mimics or miR-control were detected and compared with each other (Left) and that of the SW1088 cells with miR-544 mimics or miR-control were detected and compared with each other in the other group (Right). F. The apoptotic rate of the two glioma cell lines transfected with miR-544 mimics were measured and compared with that of the cells involving miR-controls. G. Effect of miR-544 on apoptosis in U87-2M1 cells was described using flow cytometry. H. Effect of miR-544 on apoptosis in SW1088 cells was described using flow cytometry. The square points present the relative viability in cells transfected with miR-544 mimics and the circle ones present that in the cells with miR-control. Each bar or point represents the mean of three independent experiments. Error bars represent SEM. * means $P<0.05$.

sues were measured by real-time RT-PCR respectively. As **Figure 1A** shows, the median of the relative expression levels in normal tissues was 3 but that in glioma one was 1 ($P<0.01$). To further confirm the result above, the miR-544 expressions were examined in six glioma cell lines: U87-2M1, SW1088, U87, T98G, U251 and U138. As shown in **Figure 1B**, the decreased relative levels can be observed among all these cell lines. These data indicated that miR-544 expression was downregulated in glioma tissue.

High level of miR-544 inhibits glioma cell proliferation but induce the cell apoptois

Our previous results have shown that the miR-544 expression is downregulated in both tumor tissue and cancer cell lines when compared with normal ones. So it is possible that miR-544 would have a negative effect on the proliferation of glioma cells. To test this hypothesis, two cell lines, U87-2M1 and SW1088, were transfected with miR-544 mimics which have the mature sequences of the microRNAs. The increased levels of miR-544 can be detected in the U87-2M1 and SW1088 cells after transfection (**Figure 2A**). We utilized MTT viability assays to examine the effect of miR-544 on cell proliferation. As shown in **Figure 2B** and **2C**, compared with the cells with miR-control, the cells with high level of miR-544 performed lower viability. Quantification of the assays showed that the viability of miR-544-U87-2M1 cell decreased by 0.47 fold and that of miR-544-SW1088 by 0.43 fold, compared with the cells transfected with miR-control. To uncover the effect of miR-544 on the long-term growth of glioma cells, a plate-based colony formation assays were carried out. The colony numbers of the two cell lines treated with miR-544 decreased to 48% of that of the cells with miR-control for miR-544-U87-2M1 cells and 50% for miR-544-SW1088 approximately (**Figure 2D**). Flow cytometry was used to evaluate the difference of the cell cycle distributions between the cells transfected with miR-control and that with miR-544. The G0/G1 phase fractions of miR-544-U87-2M1 and miR-544-SW1088 cells increased by 1.25 and 1.1 fold when compared with that of the transfected cells with miR-control, respectively. However, the G2/M phase fraction of the miR-544-U87-2M1 and miR-544-SW1088 cells decreased by 0.5 and 0.55 fold, respectively. The percentages of cells in S phase in transfected cells with miR-544 were lower than that in cells with miR-control (**Figure 2E**) as well. To test if the miR-544 has a positive effect on the cell apoptosis in glioma cell lines, we measured and compared the apoptosis ratios of miR-544-U87-2M1 cells with that of miR-control-U87-2M1 cells in one group, and determined and checked the apoptosis rate of miR-544-SW1088 cells against that of miR-control-SW1088 cells in the other one using flow cytometry. We discovered that the miR-544 mimic treatment on U87-2M1 cells made labeled apoptotic cells with the Annexin V or 7AAD increased by 1.45 fold and that on SW1088 cells by 1.95 fold, respectively (**Figure 2F-H**).

High level of miR-544 inhibits glioma cell migration and invasion

Transwell migration assays were exploited to examine the effect of miR-544 on cell migration and invasion. The migration level of the

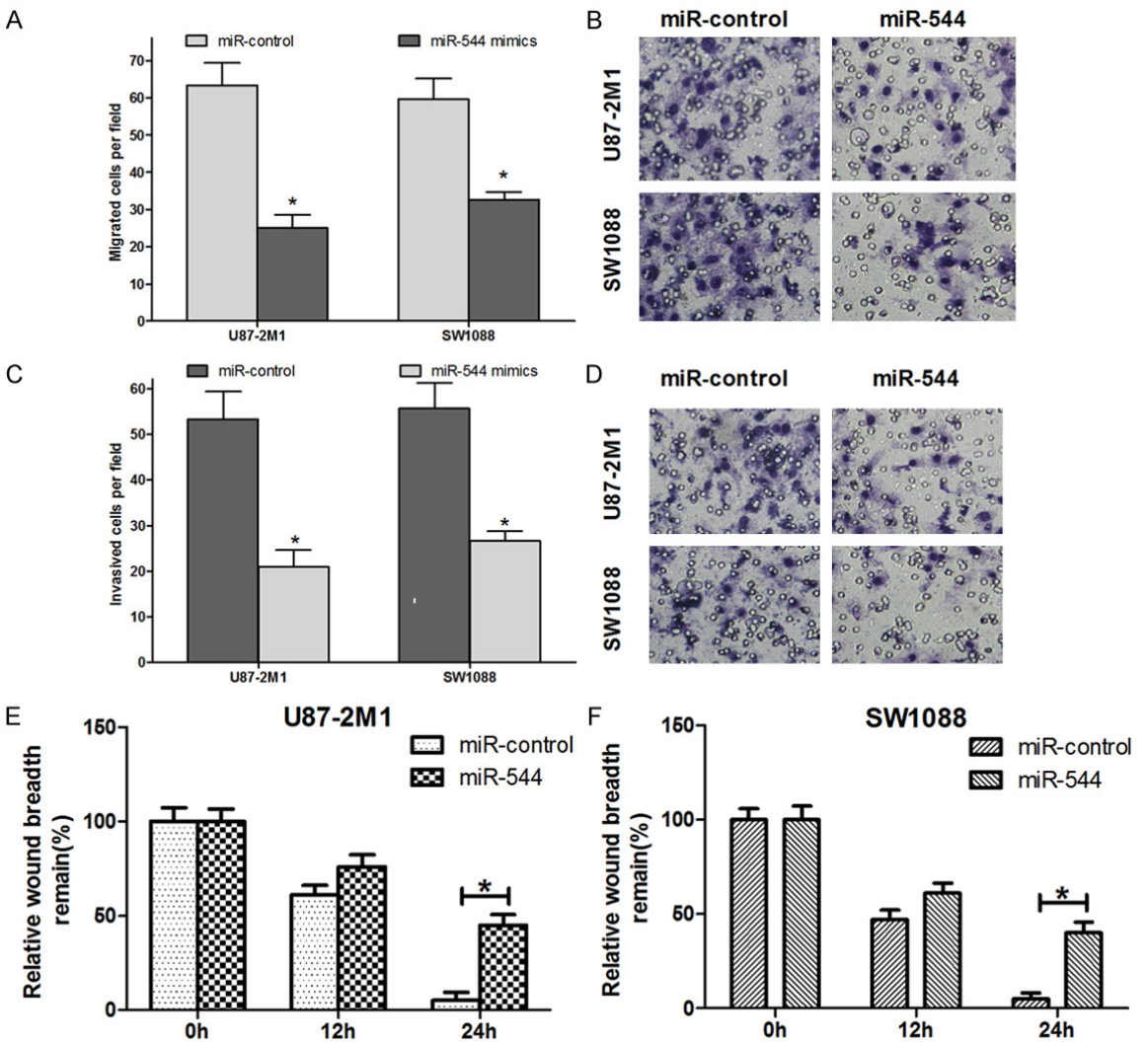

Figure 3. Overexpression of miR-544 inhibits the migration and invasion of the glioma cells in vitro. A, B. The abilities of migration of miR-544-U87-2M1 cells and that of miR-544-SW1088 cells were quantified and compared with that of the glioma cells transfected with miR-control in their respective groups (Left). The corresponding representative micrographs located on the right. C, D. The abilities of invasion of miR-544-U87-2M1 cells and that of miR-544-SW1088 cells were quantified and compared with that of the glioma cells transfected with miR-control in their respective groups (Left). The corresponding representative micrographs located on the right. E. The wound healing assay showed different cell migration in miR-544-U87-2M1 cells compared with the cells with miR-control at different time points. F. The wound healing assay showed different cell migration in miR-544-SW1088 cells compared with the cells with miR-control at different time points. The amount of motility was expressed as a percent of migration at the zero time point. Each bar represents the mean of three independent experiments. Error bars represent SEM. * means $P<0.05$.

miR-544-U87-2M1 cells reached only about 40% of that of miR-control-cells. And the migration ability of the miR-544-SW1088 cells was approximately 50% of that of the cells transfected with miR-control (**Figure 3A** and **3B**). Similarly, the transfection using miR544 made the invasive potential of the U87-2M1 cells decrease by 0.61 fold and that of the miR-544-SW1088 cells by 0.5 fold, compared with the control group, respectively (**Figure 3C** and **3D**). Furthermore, quantification of wound closure showed that miR-544-U87-2M1 cells closed 35.1% of the wound after 12 hours and 53.1% after 24 hours. However, miR-control- U87-2M1 cells closed 40.7% of the wound after 12 hours and 93.2% after 24 hours (**Figure 3E**). In the other group, miR-544-SW1088 cells closed 43.6% of the wound after 12 hours and 57.1%

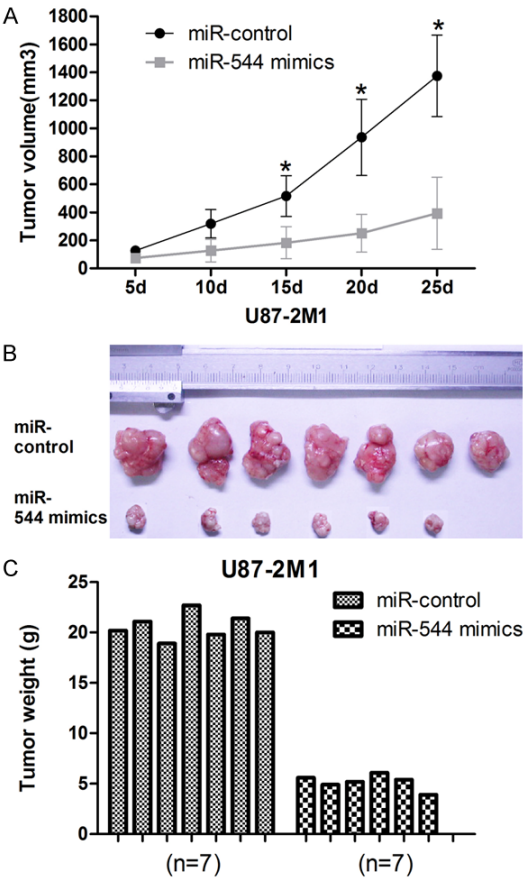

Figure 4. Overexpression of miR-544 inhibits glioma cell proliferation in vivo. A. The U87-2M1 glioma tumor growth in vivo was determined using tumor volume calculated every 5 days after injection. B. The representative image for tumor growth in vivo is shown. C. The weights of the tumors generated from the glioma cells transfected with miR-544 mimic in 7 cases of nude mices were measured and compared with the control groups. Error bars represent SEM. * means P<0.05.

after 24 hours. Meanwhile, miR-control-SW1088 cells closed 53.1% of the wound after 12 hours and 94.4% after 24 hours (**Figure 3F**). All these data above suggested the points that the increased levels of miR-544 in glioma cells significantly restrained both cell migration and invasion.

High level of miR-544 inhibits glioma cell growth in vivo

To know the role of miR-544 in glioma carcinogenesis, we further assessed the effects of increased level of miR-544 in cells on tumor growth in vivo. 3.0×10^6 of miR-544-U87-2M1 cells or miR-control-U87-2M1 cells were implanted into the right flanks of nude mice by subcutaneous injection respectively. The mean volumes of xenograft tumors were measured every 5 days. It was obviously that the tumors derived from miR-544-U87-2M1 cells were smaller than those originated from miR-control-U87-2M1 cells (n=7 animals per group, $P=3.18\times10^{-3}$) (**Figure 4A** and **4B**). At 25 days post-injection, the mean weight of the miR-544-U87-2M1 tumors was about 50% of that of miR-control-U87MG tumors (**Figure 4C**). Thus, we suggested that the transfection of miR-544 into glioma cells can inhibit the cell proliferation in vivo.

The expression of PARK7 protein is inhibited by miR-544 directly

In our study, we found that there was a negative relationship between the level of miR-544 and that of PARK7 mRNA in glioma tissues (**Figure 5A**). And a conserved binding site for miR-544 in the 3'UTR region of the PARK7 gene was identified using bioinformatical analysis (**Figure 5B**). As a result, we speculated that the expression of PARK7 in glioma cells might be negatively regulated by miR-544. To test this possibility, we firstly detected the level of PARK7 mRNA in miR-544-U87-2M1 cells and miR-544-SW1088 cells. We found that the mRNA level in these two kinds of transfected cells decreased by 0.51 fold and by 0.62, when compared with the level in their respective control group cells with miR-control (**Figure 5C** and **5D**). Furthermore, we found the increased level of PARK7 mRNA in U138 cells transfected with anti-miR-544 compared with that in the U138 cells with anti-miR-control (**Figure 5E**). Similar to the alternation of mRNA levels, the relative protein level of PARK7 in miR-544-U87-2M1 cells and miR-544-SW1088 cells were significantly lower than that in respective control group cells. Meanwhile, the amount of PARK7 protein in anti-miR-544-U138 cell was obviously larger than that in its control group cell (**Figure 5F**). To offer a more solid evidence to support our speculation, we further conducted a luciferase reporter assay. As is shown in **Figure 5G**, U872M1 or SW1088 cells cotransfected with miR-544 mimics and wild type 3'-UTR of PARK7 showed a notable decrease in luciferase activity compared to the control group. However, U872M1 or SW1088 cells co-transfected with miR-544 and mutant type 3'-UTR of PARK7

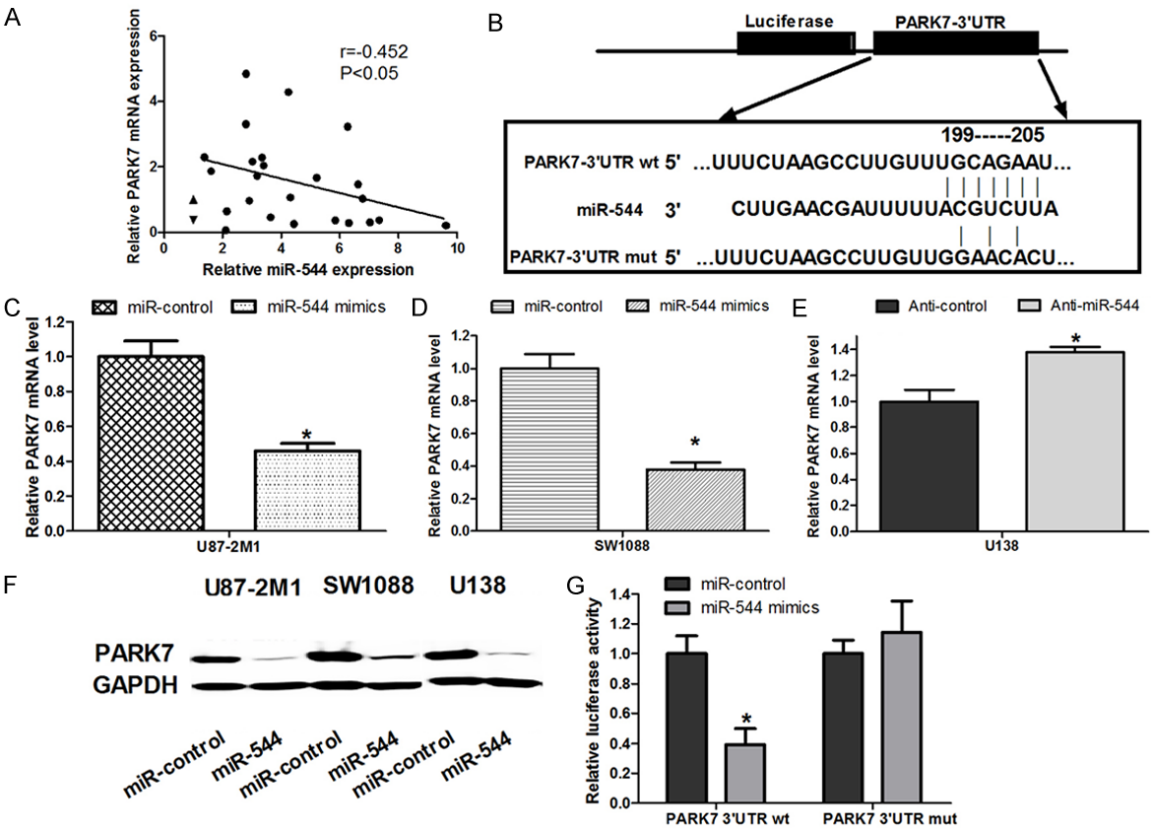

Figure 5. miR-544 targeted PARK7 by binding to its 3'-UTR. A. The correlation between miR-544 level and PARK7 mRNA level in 24 cases of glioma tissues was detected using real-time PCR. B. The sequence targeted by miR-544 in 3'-UTR of PARK7 protein (PARK7-3'UTR wt) and its corresponding mutant containing 4 mutated nucleotides (PARK7-3'UTR mut) were identified using bioinformatic analysis. C. The relative level of PARK7 mRNA was measured in U87-2M1 glioma cells transfected with miR-544 mimics or miR-control. D. The relative level of PARK7 mRNA was detected in SW1088 glioma cells transfected with miR-544 mimics or miR-control. E. The relative level of PARK7 mRNA was measured in U138 glioma cells transfected with anti-miR-544 or anti-control. F. The protein expression levels of PARK7 were detected in the cells transfected with the indicated RNA or DNA moleculars. G. U87-2M1 cells were co-transfected with miR-544 mimics and luciferase reporters containing either the predicted miRNA target site in PARK7 mRNA 3'-UTR or its corresponding mutant form. The cells co-transfected with miR-control and luciferase reporters was exploited as the control group. Error bars represent SEM. *, P < 0.05.

showed no difference in luciferase activity compared to control groups (**Figure 5G**).

MiR-544 perform its role in glioma cell development by downregulating PARK7 expression

PARK7(DJ1) protein is involved in the invasion and metastasis of the tumor cells [19, 20]. And the recent search shows that DJ-1 and β-catenin may contribute to the development and recurrence of glioma [21]. In the present research, short hairpin RNA targeting PARK7 mRNA (si-PARK7) was exploited to specifically inhibit the expression of PARK7 in miR-544-U87-2M1 cell. As is shown in **Figure 6A**, the protein level of PARK7 in the cells transfected with si-PARK7 decreased significantly compared with that in the cells with si-control by western blotting analysis. The relative level of the PARK7 protein in the U87-2M1 cells with both miR-544 mimic and the vector overexpressing the PARK7 increased by 8 fold compared with that in the cells co-tranfected with miR-544 mimic and the control vector. However, the relative amount of the protein in the U87-2M1 cells co-transfected with miR-control and the PARK7 overexpressing vector increased by only 3 fold compared with that in the group cells with miR-control and the control vector. The results above support the points that miR-544 play the same role as si-PARK7 in glioma cells and served as a negative regulator for the PARK7 expression. As shown in **Figure 6B**, inhibition of PARK7 expression by transfection with si-PARK7 or miR-544

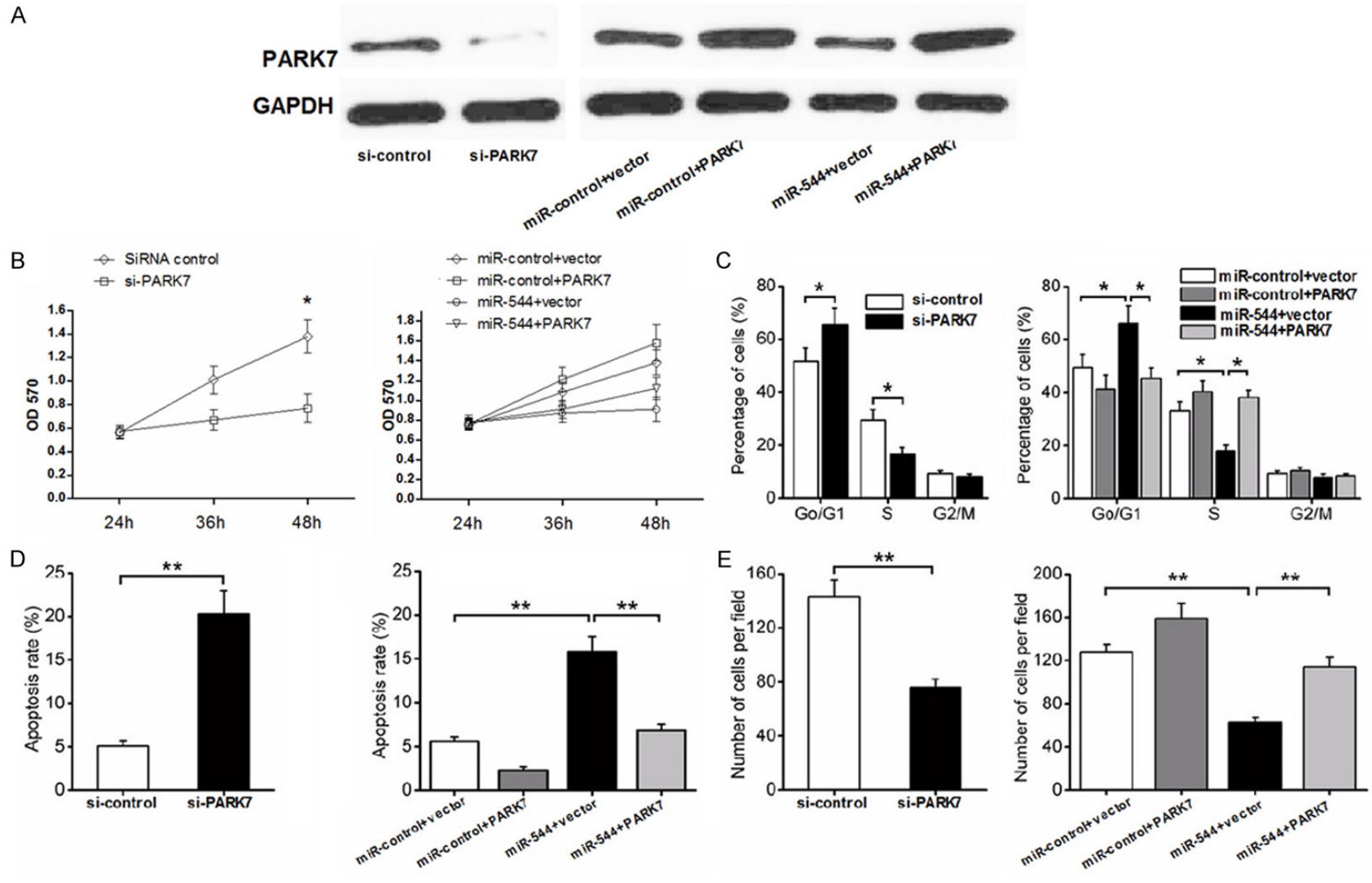

Figure 6. A. The levels of PARK7 expression in U87-2M1 cells after the transfection of si-PARK7 or the co-transfection of miR-544 and the vector overexpressing the PARK7 protein were measured and compared with the control group indicated in Figures. B. The effect of the si-PARK7 or miR-544 mimics transfection on the viability of glioma cells that related to the PARK7 expression was detected using MTT assays. C. The effect of the si-PARK7 or miR-544 mimics transfection on the cell cycle of glioma cells that related to the PARK7 expression was detected using flow cytometry. D. The effect of the si-PARK7 or miR-544 mimics transfection on the apoptosis of glioma cells that related to the PARK7 expression was detected using flow cytometry. E. The effect of the si-PARK7 or miR-544 mimics transfection on the migration of glioma cells that related to the PARK7 expression was detected using transwell assays. Each bar represents the mean of three independent experiments. Error bars represent SEM. * means $P<0.05$, ** means $P<0.01$.

decreased U87-2M1 cell viability, while the overexpression of PARK7 reversed the suppressive effect of miR-544 on U87-2M1 cell viability partially. The G0/G1 phase fractions increased but the S and G2/M phase fractions decreased as the PARK7 expression was inhibited by the si-PARK7 or miR-544 transfected into the cells. And the overexpression of PARK7 in miR-544-U87-2M1 cells made phase fractions return to the similar level as that in control group cells with miR-control and the control vector by counteracting the effect of miR-544 on the glioma cell cycle in part (**Figure 6C**). In a similar manner, si-PARK7 or miR-544 increased the apoptotic rate of U87-2M1 cells and inhibited the cell migration by suppressing the expression of PARK7. Meanwhile, the overexpression of PARK7 canceled the effect of miR-544 on cell apoptosis and cell migration out (**Figure 6D** and **6E**). These findings suggest that miR-544 promotes glioma cell proliferation and inhibits its apoptosis, partially through targeting PARK7.

Discussion

Gliomas have been categorized according to their grade. Low-grade gliomas are well differentiated and grow slowly but show a consistent tendency to diffusely infiltrate the surrounding brain tissue. And the median survival time of patients with anaplastic astrocytomas is less than 3 years, while for glioblastoma this is less than one year [22, 23]. It has been described that the expression levels of miR-544 decreased significantly in anaplastic gliomas or glioblastoma compared with low-grade gliomas [24]. Consistent with the previous result reported, we found that miR-544 were significantly downregulated in glioma tissues when compared with adjacent normal tissue. The proliferation and the ability of migration and invasion of the glioma cells become abated as the level of miR-544 was increased (**Figure 3A-D**). However, the apoptosis rate of glioma cells with high level of miR-544 decreased. On the basis of these results, we considered that miR-544 may serve as a negative regulator in the tumorigenesis and development of gliomas. The further research showed that miR-544 dramatically decreased the level of PARK7 mRNA and inhibited the protein expression in glioma cells by binding to the complementary sites within the 3'-UTR of PARK7 directly (**Figure 5B-G**).

The gene encoding Parkinson Protein 7 which is also known as DJ1 was originally identified as an oncogene that transforms NIH3T3 cells in cooperation with the activated Ras gene [25]. Recent studies have demonstrated that the gene is expressed at a high level in breast cancer, lung cancer, prostate cancer and ovarian cancer [26, 27]. PARK7 regulates cell cycle progression or inhibits the cell apoptosis by binding to p53BP3, p53 [28], DAXX (death domain-associated protein), ASK1 (Apoptosis signal-regulating kinase 1) [29, 30] and PTEN (Phosphatase with tensin homology) [31]. It has been recently recorded that the protein acts as an EMT-positive regulator in breast cancer cells via regulation of the KLF17/ID-1 pathway [32] and the protein underexpression significantly inhibited invasion and migration of gastric cancer cells [33]. In accordance with the previous results described in other cell lines, we found that the knockdown of PARK7 protein using the transfection of si-PARK7 into U87-2M1 glioma cells inhibits the cell proliferation through increasing the percentage of G1/G0 phase cells but decreasing that of S or G2/M phase cells, and promotes the cell apoptosis to play a negative role in the development of tumor cells (**Figure 6B-E**).

The majority of microRNAs are known to regulate target mRNAs by binding to the 3'-UTR of target gene in a post-transcriptional manner [6]. A target sequence of miR-544 on the 3'UTR of PARK7 mRNA was identified using Targetscan 5.0 and demonstrated according to the decreased level of PARK7 mRNA and protein in glioma cells after the transfection of miR-544 mimics. The direct targeting was further supported through luciferase reporter assay. The effect of miR-544 on the glioma cell proliferation, migration and invasion and cell apoptosis were similar to that of si-PARK7 and significantly attenuated by the overexpression of PARK7 (**Figure 6B-E**). As a result, it is reasonable that miR-544 inhibit glioma cell proliferation and migration but induce cell apoptosis by suppressing the PARK7 expression. The negative role of miR-544 in tumor growth may provide a possibility to treat gliomas using a new strategy in the future.

Acknowledgements

We thank the fund support from Jiangsu province twelfth five-year (science, education and

health project) innovation team and talents (IJ201159); Jiangsu province science and technology support plan-social development project (BE02010697); National Program on Key Basic Research Projects (973 Program, 2007-CB936104)

Disclosure of conflict of interest

None.

Address correspondence to: Daxin Wang, Northern Jiangsu People's Hospital, Yangzhou 225001, Jiangsu, China. Tel: 0514-87937541; Fax: 0514-87937541; E-mail: wangdaxin101@163.com

References

[1] Mamelak AN and Jacoby DB. Targeted delivery of antitumoral therapy to glioma and other malignancies with synthetic chlorotoxin (TM-601). Expert Opin Drug Deliv 2007; 4: 175-186.

[2] Goodenberger ML and Jenkins RB. Genetics of adult glioma. Cancer Genet 2012; 205: 613-621.

[3] Kanu OO, Hughes B, Di C, Lin N, Fu J, Bigner DD, Yan H and Adamson C. Glioblastoma Multiforme Oncogenomics and Signaling Pathways. Clin Med Oncol 2009; 3: 39-52.

[4] Ostrom QT and Barnholtz-Sloan JS. Current state of our knowledge on brain tumor epidemiology. Curr Neurol Neurosci Rep 2011; 11: 329-335.

[5] Bartel DP. MicroRNAs: genomics, biogenesis, mechanism, and function. Cell 2004; 116: 281-297.

[6] Hwang HW and Mendell JT. MicroRNAs in cell proliferation, cell death, and tumorigenesis. Br J Cancer 2007; 96 Suppl: R40-44.

[7] Ambros V. The functions of animal microRNAs. Nature 2004; 431: 350-355.

[8] Yang L, Li Q, Wang Q, Jiang Z and Zhang L. Silencing of miRNA-218 promotes migration and invasion of breast cancer via Slit2-Robo1 pathway. Biomed Pharmacother 2012; 66: 535-540.

[9] Chan JA, Krichevsky AM and Kosik KS. MicroRNA-21 is an antiapoptotic factor in human glioblastoma cells. Cancer Res 2005; 65: 6029-6033.

[10] Kloosterman WP and Plasterk RH. The diverse functions of microRNAs in animal development and disease. Dev Cell 2006; 11: 441-450.

[11] Yang L, Wang YL, Liu S, Zhang PP, Chen Z, Liu M and Tang H. miR-181b promotes cell proliferation and reduces apoptosis by repressing the expression of adenylyl cyclase 9 (AC9) in cervical cancer cells. FEBS Lett 2014; 588: 124-130.

[12] Ciafre SA, Galardi S, Mangiola A, Ferracin M, Liu CG, Sabatino G, Negrini M, Maira G, Croce CM and Farace MG. Extensive modulation of a set of microRNAs in primary glioblastoma. Biochem Biophys Res Commun 2005; 334: 1351-1358.

[13] Gabriely G, Yi M, Narayan RS, Niers JM, Wurdinger T, Imitola J, Ligon KL, Kesari S, Esau C, Stephens RM, Tannous BA and Krichevsky AM. Human glioma growth is controlled by microRNA-10b. Cancer Res 2011; 71: 3563-3572.

[14] Papagiannakopoulos T, Shapiro A and Kosik KS. MicroRNA-21 targets a network of key tumor-suppressive pathways in glioblastoma cells. Cancer Res 2008; 68: 8164-8172.

[15] Tu Y, Gao X, Li G, Fu H, Cui D, Liu H, Jin W and Zhang Y. MicroRNA-218 inhibits glioma invasion, migration, proliferation, and cancer stem-like cell self-renewal by targeting the polycomb group gene Bmi1. Cancer Res 2013; 73: 6046-6055.

[16] Hui W, Yuntao L, Lun L, WenSheng L, ChaoFeng L, HaiYong H and Yueyang B. MicroRNA-195 inhibits the proliferation of human glioma cells by directly targeting cyclin D1 and cyclin E1. PLoS One 2013; 8: e54932.

[17] Sun G, Cao Y, Shi L, Sun L, Wang Y, Chen C, Wan Z, Fu L and You Y. Overexpressed miRNA-137 inhibits human glioma cells growth by targeting Rac1. Cancer Biother Radiopharm 2013; 28: 327-334.

[18] Yang TQ, Lu XJ, Wu TF, Ding DD, Zhao ZH, Chen GL, Xie XS, Li B, Wei YX, Guo LC, Zhang Y, Huang YL, Zhou YX and Du ZW. MicroRNA-16 inhibits glioma cell growth and invasion through suppression of BCL2 and the nuclear factor-kappaB1/MMP9 signaling pathway. Cancer Sci 2014; 105: 265-271.

[19] He X, Zheng Z, Li J, Ben Q, Liu J, Zhang J, Ji J, Yu B, Chen X, Su L, Zhou L, Liu B and Yuan Y. DJ-1 promotes invasion and metastasis of pancreatic cancer cells by activating SRC/ERK/uPA. Carcinogenesis 2012; 33: 555-562.

[20] Bai J, Guo C, Sun W, Li M, Meng X, Yu Y, Jin Y, Tong D, Geng J, Huang Q, Qi J and Fu S. DJ-1 may contribute to metastasis of non-small cell lung cancer. Mol Biol Rep 2012; 39: 2697-2703.

[21] Wang C, Fang M, Zhang M, Li W, Guan H, Sun Y, Xie S and Zhong X. The positive correlation between DJ-1 and beta-catenin expression shows prognostic value for patients with glioma. Neuropathology 2013; 33: 628-636.

[22] Watanabe K, Sato K, Biernat W, Tachibana O, von Ammon K, Ogata N, Yonekawa Y, Kleihues P and Ohgaki H. Incidence and timing of p53 mutations during astrocytoma progression in

patients with multiple biopsies. Clin Cancer Res 1997; 3: 523-530.
[23] Stupp R, Reni M, Gatta G, Mazza E and Vecht C. Anaplastic astrocytoma in adults. Crit Rev Oncol Hematol 2007; 63: 72-80.
[24] Ma R, Zhang G, Wang H, Lv H, Fang F and Kang X. Downregulation of miR-544 in tissue, but not in serum, is a novel biomarker of malignant transformation in glioma. Oncol Lett 2012; 4: 1321-1324.
[25] Nagakubo D, Taira T, Kitaura H, Ikeda M, Tamai K, Iguchi-Ariga SM and Ariga H. DJ-1, a novel oncogene which transforms mouse NIH3T3 cells in cooperation with ras. Biochem Biophys Res Commun 1997; 231: 509-513.
[26] Tsuchiya B, Iwaya K, Kohno N, Kawate T, Akahoshi T, Matsubara O and Mukai K. Clinical significance of DJ-1 as a secretory molecule: retrospective study of DJ-1 expression at mRNA and protein levels in ductal carcinoma of the breast. Histopathology 2012; 61: 69-77.
[27] Bindukumar B, Schwartz S, Aalinkeel R, Mahajan S, Lieberman A and Chadha K. Proteomic profiling of the effect of prostate-specific antigen on prostate cancer cells. Prostate 2008; 68: 1531-1545.
[28] Shinbo Y, Taira T, Niki T, Iguchi-Ariga SM and Ariga H. DJ-1 restores p53 transcription activity inhibited by Topors/p53BP3. Int J Oncol 2005; 26: 641-648.
[29] Karunakaran S, Diwakar L, Saeed U, Agarwal V, Ramakrishnan S, Iyengar S and Ravindranath V. Activation of apoptosis signal regulating kinase 1 (ASK1) and translocation of death-associated protein, Daxx, in substantia nigra pars compacta in a mouse model of Parkinson's disease: protection by alpha-lipoic acid. FASEB J 2007; 21: 2226-2236.
[30] Junn E, Taniguchi H, Jeong BS, Zhao X, Ichijo H and Mouradian MM. Interaction of DJ-1 with Daxx inhibits apoptosis signal-regulating kinase 1 activity and cell death. Proc Natl Acad Sci U S A 2005; 102: 9691-9696.
[31] Kim RH, Peters M, Jang Y, Shi W, Pintilie M, Fletcher GC, DeLuca C, Liepa J, Zhou L, Snow B, Binari RC, Manoukian AS, Bray MR, Liu FF, Tsao MS and Mak TW. DJ-1, a novel regulator of the tumor suppressor PTEN. Cancer Cell 2005; 7: 263-273.
[32] Ismail IA, Kang HS, Lee HJ, Kim JK and Hong SH. DJ-1 upregulates breast cancer cell invasion by repressing KLF17 expression. Br J Cancer 2014; 110: 1298-1306.
[33] Zhu ZM, Li ZR, Huang Y, Yu HH, Huang XS, Yan YF, Shao JH and Chen HP. DJ-1 is involved in the peritoneal metastasis of gastric cancer through activation of the Akt signaling pathway. Oncol Rep 2014; 31: 1489-1497.